Few-Body Systems 7, 95–117 (1989)

Few-Body Systems

Deuteron Photodisintegration with the Bonn OBE Potentials*

K.-M. Schmitt and H. Arenhövel

Institut für Kernphysik, Johannes-Gutenberg-Universität Mainz, J.-J.-Becher-Weg 45, D-6500 Mainz, Federal Republic of Germany

Abstract. The various OBE approximations to the recent Bonn potential are studied in deuteron photodisintegration below π-threshold. Consistent static meson-exchange currents, isobar currents, and the relativistic spin-orbit current are included. Concerning the OBEPT also the leading retardation corrections in the currents are taken into account. Comparison with experimental data is carried out in detail.

1 Introduction

The role of deuteron photodisintegration as a testing ground for new theoretical concepts of the strong interaction has a long history in nuclear physics [1]. Recently, Machleidt et al. [2] presented a comprehensive field theoretical model of the N-N interaction below π-threshold including all diagrams up to an exchange energy of order of the cut-off masses. In addition to their very successful "full model", which contains no fictitious exchange terms and as phenomenological input only masses, coupling constants, and form factors, they also gave various approximations to the "full model" in terms of simple one-boson exchanges. Since these OBE potentials are acceptable, in retaining the most important features of the "full model" on the one hand and being quite easily applicable in momentum-space calculations on the other hand, it seems legitimate to investigate them in further detail by studying them in deuteron photodisintegration. This will be the simplest test case for these OBEPs, which goes beyond their pure hadronic features, the extension in terms of interaction currents being included implicitly in these potentials via minimal coupling of the electromagnetic field.

In Sect. 2 we will first outline the formalism for the solution of the Lippmann-Schwinger equations in $(ls)j$-basis for the different OBEPs considered, namely the relativistic OBEPQ, the time-dependent OBEPT, and the nonrelativistic OBEPR. Then we collect the corresponding electromagnetic currents which we will consider for photodisintegration of the deuteron. Concerning the meson-exchange currents we construct the dominant parts consistently with the given potentials. The effects

* Supported by Deutsche Forschungsgemeinschaft (SFB 201)

of additional MEC, not included in our set of explicit currents, will be estimated by the use of the Siegert operators in different gauges. In the case of the retarded OBEPT we construct the corresponding leading retardation corrections to the MEC in an expansion of the retarded propagators with respect to the ratio (nucleon kinetic energy)/(pion mass) following the formalism of ref. [3]. For a realistic comparison with experimental data we include in addition the relativistic spin-orbit current [4] and isobar currents. For the latter it is sufficient to take them in the impulse approximation. Finally, also lowest-order relativistic corrections to the one-body currents will be considered.

In Sect. 3 we compare the OBEP predictions for deuteron photodisintegration below π-threshold with experimental data for the unpolarized cross section and a few polarization observables already measured, i.e. the photon asymmetry and the neutron polarization. Furthermore, additional polarization observables are calculated with respect to their possible role of differentiating between different theoretical models. A summary is given in Sect. 4.

2 Theoretical Models

In the following we will consider the three OBE approximations to the Bonn "full model":

(i) The *OBEPQ* is essentially constructed from the "full model" by neglecting any contributions but pure OBE terms. Furthermore, the energy dependence of the OBE propagators is neglected by using the Blankenbecler-Sugar reduction [5] of the Bethe-Salpeter equation [6].

(ii) The *OBEPT* can be obtained from the OBEPQ by (a) restoring the energy dependence in the propagators, (b) leaving out the factors of minimal relativity, and (c) neglecting a certain off-shell term in the vector-meson part.

(iii) The *OBEPR* is obtained from the OBEPQ by a non-relativistic reduction of the nucleon-meson vertices up to order p^2/m^2. It is formally equivalent to the former BS-III-potential [7], if minimal relativity is included therein.

By keeping the parameters of the crucial mesons (π, ρ, ω) almost the same as in the "full model", Machleidt et al. demonstrated that these OBEPs are acceptable approximations to the "full model". This concerns the phase shifts for not too high energies as well as the low-energy parameters. Especially the feature of combining a low D-state probability of the deuteron wave function with a realistic quadrupole moment is perserved for these OBEPs, as far as it is possible for the energy-independent ones.

Despite the fact that the OBEPR is specifically constructed for r-space calculations, it is more convenient for our purpose of treating all three OBEPs on the same level, i.e. to work in p-space also in the case of the OBEPR. For any of the OBEPs considered, the N-N wave equations to be solved are of Lippmann-Schwinger type, where for the OBEPT the potential is energy-dependent. Technical aspects of the solution of the LS-equations for the deuteron and the scattering states in $(ls)j$-basis, which we have used, are summarized in ref. [8]. The necessary partial-wave amplitudes for the OBEPs are given in the Appendix. Since we calculate the current matrix elements for deuteron photodisintegration in r-space, a numerical Fourier transfor-

mation of wave functions from p- to r-space is necessary. Details can also be found in ref. [8].

We will start the discussion of currents with the pionic exchange current. One might argue that in order to be completely consistent with the corresponding pionic part of the potential, for example Eq. (A.2) for the OBEPQ, one should apply the standard method of minimal coupling. The rather extensive technical problems of such an attempt could be overcome in a pure p-space calculation, i.e., if one does not need to represent the electromagnetic currents in configuration space as we do. But apart from these technical problems there are good justifications for avoiding these complications: First, any contributions in Eq. (A.2) going beyond the static limit are genuine relativistic effects of order of at least p^4/m^4. Even if such corrections to the potential turn out to be non-negligible as they manifestly show up in the deuteron wave function for example, their significance would be unclear in the two-body break-up process as long as one has not included all corresponding relativistic corrections up to the same order. Secondly, since the potential of Eq. (A.2) appears only formally in the N-N LS-equation but has been retained in the BbS-reduction of the BS-equation, the method of minimal coupling would not be appropriate for the higher-order terms. With respect to the first point we like to emphasize that we do not aim at a complete relativistic description. For example, we calculate both the deuteron and the final N-N scattering state in their center-of-mass frames, assuming the center-of-mass motion being independent of the relative motion, which is justified only non-relativistically. The actual reason, however, why we proceed as below is the fact that we will be able to demonstrate the possibility to neglect higher-order corrections in the current by use of the Siegert operator in different gauges, at least for the energy region we are interested in.

Taking henceforth only the lowest order of an expansion of Eq. (A.2) in powers of p^2/m^2 and using the relation (A.1) one obtains the well-known static pion-exchange potential

$$\hat{V}_\pi = \frac{g_\pi^2}{4\pi}\frac{1}{4m^2}\vec{\tau}_1\cdot\vec{\tau}_2[\vec{\sigma}_1\cdot\hat{\vec{p}}_1, [\vec{\sigma}_2\cdot\hat{\vec{p}}_2, J_\pi^{\mathrm{reg}}(|\hat{\vec{r}}|)]] \tag{2.1}$$

($\vec{r} = \vec{r}_1 - \vec{r}_2$), from which the corresponding static pion-exchange current follows by minimal coupling,

$$\begin{aligned}\hat{\vec{j}}_\pi(\vec{x}) = &-ie\frac{g_\pi^2}{4\pi}\frac{1}{4m^2}(\vec{\tau}_1\times\vec{\tau}_2)_0\\ &*\Big\{\vec{\sigma}_1\delta(\vec{x}-\hat{\vec{r}}_1)[\vec{\sigma}_2\cdot\hat{\vec{p}}_2, J_\pi^{\mathrm{reg}}(|\vec{x}-\hat{\vec{r}}_2|)]\\ &-\vec{\sigma}_2\delta(\vec{x}-\hat{\vec{r}}_2)[\vec{\sigma}_1\cdot\hat{\vec{p}}_1, J_\pi^{\mathrm{reg}}(|\vec{x}-\hat{\vec{r}}_2|)]\\ &+\frac{i}{4\pi}[\vec{\sigma}_1\cdot\hat{\vec{p}}_1, [\vec{\sigma}_2\cdot\hat{\vec{p}}_2, (J(|\vec{x}-\hat{\vec{r}}_1|;m_\pi)\overleftrightarrow{\nabla}_{\vec{x}}J(|\vec{x}-\hat{\vec{r}}_2|;m_\pi)^{\mathrm{reg}}]]\Big\}.\end{aligned} \tag{2.2}$$

What we now mean by consistency of the currents essentially concerns the consistent incorporation of hadronic form factors as provided by the OBEPs into the currents. The static meson propagator appearing in Eq. (2.1) can be written for an arbitrary meson α (with mass m_α and cut-off Λ_α) as

$$J_\alpha^{\text{reg}}(|\vec{r}|) = \frac{4\pi}{(2\pi)^3} \int d^3Q \, e^{i\vec{Q}\cdot\vec{r}} \frac{F_\alpha^2(\vec{Q}^2)}{\omega_{\vec{Q}}^2}, \tag{2.3}$$

with $\omega_{\vec{Q}} = (\vec{Q}^2 + m_\alpha^2)^{1/2}$, and the form factor

$$F_\alpha(\vec{Q}^2) = \left(\frac{\Lambda_\alpha^2 - m_\alpha^2}{\Lambda_\alpha^2 + \vec{Q}^2}\right)^{n_\alpha}. \tag{2.4}$$

Calling $I_\alpha = 2n_\alpha$ the regularization order of the corresponding potential part, the ρ-meson in the OBEPQ carries a quadrupole regularization ($I_\alpha = 4$), whereas all other mesons included in the OBEPQ, and all mesons in OBEPT and OBEPR have dipole form factors ($I_\alpha = 2$). For the contact or pair-current part of the static π-MEC of Eq. (2.2) we therefore use

$$J_\pi^{\text{reg}}(|\vec{r}|) = J(r; m_\pi) - J(r; \Lambda_\pi) - (1 - b_\pi^2)\tfrac{1}{2}\Lambda_\pi e^{-\Lambda_\pi r}, \tag{2.5}$$

with $b_\alpha = m_\alpha/\Lambda_\alpha$, and the unregularized static propagator ($I_\alpha = 0$) is given by

$$J(r; m_\alpha) = \frac{e^{-m_\alpha r}}{r}. \tag{2.6}$$

Eq. (2.5) is a special case of the more general fact that, given an operator $F(m_\alpha^2)$ as for example a static OBEP, a static MEC or a static propagator coefficient like in Eq. (A.15) the corresponding properly regularized operator $F^{\text{reg}}(m_\alpha^2, \Lambda_\alpha^2, I_\alpha)$ is given by

$$F^{\text{reg}}(m_\alpha^2, \Lambda_\alpha^2, I_\alpha) = F(m_\alpha^2) - \sum_{k=0}^{I_\alpha - 1} \frac{1}{k!}(m_\alpha^2 - \Lambda_\alpha^2)^k \frac{d^k}{d(\Lambda_\alpha^2)^k} F(\Lambda_\alpha^2), \tag{2.7}$$

if a form factor of the type of Eq. (2.4) is assumed. Eq. (2.7) has to be used for the true exchange part of the static π-MEC of Eq. (2.2), and it follows from Eq. (2.7) how the functions $\Phi'^{(v)}_{\sigma,L}$ (defined in ref [9]) appearing in a multipole decomposition have to be changed for consistency.

The next current we take explicitly into account is the static ρ-MEC. As for the pion case we only take the lowest order in p^2/m^2 of Eq. (A.4), but in addition we restrict ourselves to the leading terms in an expansion of g_ρ/f_ρ, the ratio of vector- to tensor-coupling constant, which is chosen to be $(6.1)^{-1} \ll 1$ for any of the three OBEPs. From Eq. (A.1) one obtains for this dominant part of the static ρ-exchange potential

$$\hat{V}_\rho = \frac{(g_\rho + f_\rho)^2}{4\pi} \frac{1}{4m^2} \vec{\tau}_1 \cdot \vec{\tau}_2 [(\vec{\sigma}_1 \times \hat{\vec{p}}_1); [\vec{\sigma}_2 \times \hat{\vec{p}}_2, J_\rho^{\text{reg}}(|\hat{\vec{r}}|)]], \tag{2.8}$$

from which minimal coupling gives the corresponding dominant static ρ-exchange current

$$\begin{aligned}
\hat{\vec{j}}_\rho(\vec{x}) = &-ie\frac{(g_\rho + f_\rho)^2}{4\pi} \frac{1}{4m^2} (\vec{\tau}_1 \times \vec{\tau}_2)_0 \\
&* \Big\{ -\delta(\vec{x} - \hat{\vec{r}}_1)\vec{\sigma}_1 \times [\vec{\sigma}_2 \times \hat{\vec{p}}_2, J_\rho^{\text{reg}}(|\vec{x} - \hat{\vec{r}}_2|)] \\
&+ \delta(\vec{x} - \hat{\vec{r}}_2)\vec{\sigma}_2 \times [\vec{\sigma}_1 \times \hat{\vec{p}}_1, J_\rho^{\text{reg}}(|\vec{x} - \hat{\vec{r}}_1|)] \\
&+ \frac{i}{4\pi} [\vec{\sigma}_1 \times \hat{\vec{p}}_1; [\vec{\sigma}_2 \times \hat{\vec{p}}_2, (J(|\vec{x} - \hat{\vec{r}}_1|; m_\rho) \overleftrightarrow{\nabla}_{\vec{x}} J(|\vec{x} - \hat{\vec{r}}_2|; m_\rho))^{\text{reg}}]] \Big\}.
\end{aligned} \tag{2.9}$$

Note that, besides retardation corrections in the meson propagators for the OBEPT, which are discussed below, the π- and ρ-MEC of Eqs. (2.2) and (2.9) are the same, except for meson parameters and form factors, for OBEPQ, -T and -R, since the differences in the meson-nucleon vertices and in the factors of minimal relativity are of higher order (see the Appendix).

To demonstrate the necessity for including the ρ-MEC of Eq. (2.9) in a calculation with explicit currents only, i.e. without Siegert operators, we show in Fig. 1 the differential cross sections for deuteron photodisintegration in the c.m.-system at 100 MeV photon laboratory energy for the different OBEPs with and without this ρ-MEC. (The nomenclature for current contributions used in Fig. 1 and further

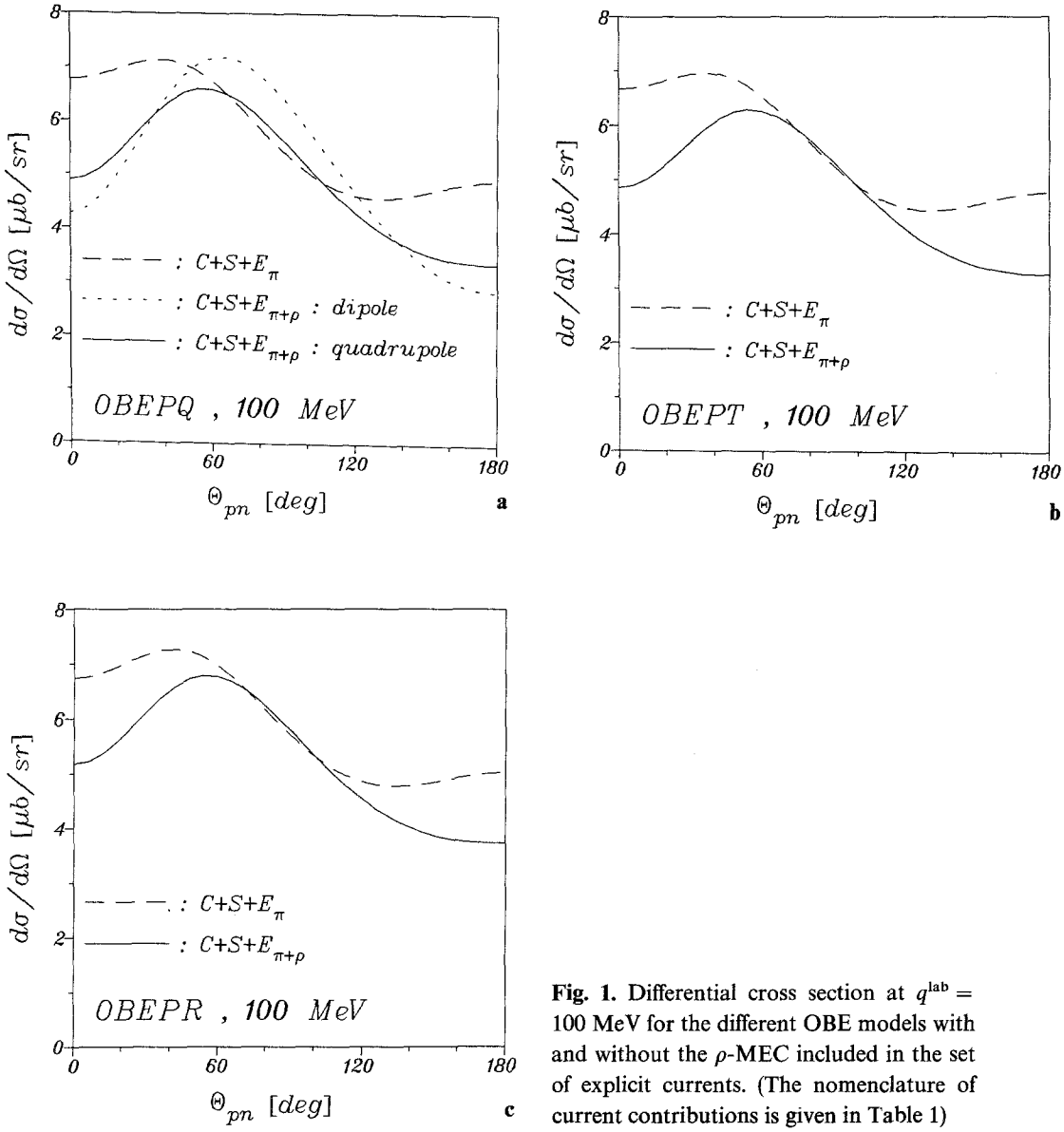

Fig. 1. Differential cross section at $q^{\text{lab}} =$ 100 MeV for the different OBE models with and without the ρ-MEC included in the set of explicit currents. (The nomenclature of current contributions is given in Table 1)

Table 1. Nomenclature for the current contributions used in Figs. 1 a–c, 2, 5, 6

C	Convection current (Eq. (4.16) of ref. [3])
S	Spin current (Eq. (4.17) of ref. [3])
E	Static MEC (Eq. (2.2) for π- and Eq. (2.9) for ρ-part)
SO	Relativistic spin-orbit current (Eq. (2) of ref. [16])
IC	One-body isobar current (Eqs. (58)–(63) of ref. [22])
R	Relativistic one-body current (Eq. (4.18) of ref. [3])
e	Retardation corrections to π- and ρ-MEC

on is summarized in Table 1.) The influence is quite dramatic, especially for small and large angles, but very similar for the different potentials. In the OBEPQ case the consistent quadrupole-regularized ρ-MEC is compared to a dipole version. The substantial difference again underlines the importance of consistency of the MEC with the given potential. Of course, the non-relativistic one-body current, i.e. convection and spin current, are always included.

To estimate the contributions of exchange currents beyond the dominant π- and ρ-MEC we now use the Siegert operators in different gauges. Following ref. [10], the transverse electric multipole operator

$$\hat{T}^{[L]}_{\mathrm{el}}(q;\hat{\vec{j}}) = \int d^3x\, \vec{A}^{[L]}_{\mathrm{el}}(\vec{x}, q)\cdot\hat{\vec{j}}(\vec{x}), \tag{2.10}$$

with

$$\vec{A}^{[L]}_{\mathrm{el}}(\vec{x}, q) = \frac{i}{\hat{L}}(\sqrt{L+1}\, j_{L-1}(z)\vec{Y}^{[L]}_{L-1}(\hat{x}) - \sqrt{L}\, j_{L+1}(z)\vec{Y}^{[L]}_{L+1}(\hat{x})) \tag{2.11}$$

($z = qx$, $x = |\vec{x}|$, $\hat{x} = \vec{x}/x$), may be split in two parts

$$\hat{T}^{[L]}_{\mathrm{el}}(q;\hat{\vec{j}}) = \hat{T}^{[L]}_{a}(q;\hat{\vec{j}}) + \hat{T}^{[L]}_{b}(q;\hat{\vec{j}}), \tag{2.12}$$

according to the decomposition

$$\vec{A}^{[L]}_{\mathrm{el}} = \vec{\nabla}\Phi^{[L]} + (\vec{A}^{[L]}_{\mathrm{el}} - \vec{\nabla}\Phi^{[L]}). \tag{2.13}$$

For a sufficiently localized current density and not too high photon energies, $\hat{T}^{[L]}_{a}$ will give the major contribution for any choice of

$$\Phi^{[L]}(\vec{x}, q) = \frac{i}{\sqrt{L(L+1)}}\frac{1}{q}\left(\frac{L+1}{(2L+1)!!}z^L + \varphi_L(z)\right)Y^{[L]}(\hat{x}), \tag{2.14}$$

where φ_L is an arbitrary function except that it should satisfy the limit

$$\varphi_L(z) \underset{z\to 0}{\to} \mathcal{O}(z^{L+2}). \tag{2.15}$$

Because of this condition $\vec{A}^{[L]}_{\mathrm{el}} - \vec{\nabla}\Phi^{[L]}$ is two orders in z higher than $\vec{\nabla}\Phi^{[L]}$, and correspondingly the contributions of $\hat{T}^{[L]}_{a}$ will dominate over $\hat{T}^{[L]}_{b}$ at low momentum transfer. Different choices of φ_L can be connected via gauge transformations, and we will consider the following cases,

$$
\begin{aligned}
n_s = 0: &\quad \varphi_L(z) = 0, \\
n_s = 1: &\quad \varphi_L(z) = \left(1 + z\frac{d}{dz}\right) j_L(z) - \frac{L+1}{(2L+1)!!} z^L, \\
n_s = 2: &\quad \varphi_L(z) = (L+1) j_L(z) - \frac{L+1}{(2L+1)!!} z^L, \\
n_s = 3: &\quad \varphi_L(z) = \frac{L+1}{(2L+1)!!} z^L (g_L(z) - 1).
\end{aligned} \tag{2.16}
$$

The number n_s will be used for labelling the corresponding Siegert operators. $n_s = 1$ and $n_s = 2$ denote the frequently used Partovi [11] and standard gauges and the recent Friar-Fallieros [12] gauge is denoted by $n_s = 3$. The least sophisticated and simplest choice is what we will call the z^L-gauge ($n_s = 0$).

Application of the Siegert theorem (ST) means to evaluate $\hat{T}_a^{[L]}$ via the charge density (i.e. the one-body charge density according to Siegert's hypothesis [10]) using current conservation

$$
\hat{T}_a^{[L]}(q; \hat{\vec{j}}) = i \int d^3x \, [\hat{H}, \hat{\rho}(\vec{x})] \Phi^{[L]}(\vec{x}, q), \tag{2.17}
$$

while for $\hat{T}_b^{[L]}$ the explicitly constructed currents are used. If the current in $\hat{T}_b^{[L]}$ is restricted to its one-body part, we will call this the normal part [10] of $\hat{T}_{el}^{[L]}$. The normal part of the magnetic multipoles include the one-body current only. If the two-body part of the current in $\hat{T}_b^{[L]}$ is not completely consistent to the potential, gauge invariance is not fulfilled and the gauge dependence of the results will indicate the inconsistency.

As an example we consider the differential cross section at $q^{\text{lab}} = 100$ MeV for the OBEPR in Fig. 2. The long-dashed curve is identical to the solid curve of Fig. 1 c. The solid curve of Fig. 2 corresponds to a calculation with ST in z^L-gauge. Also the normal parts according to (2.16) are shown. Thus, additional MEC beyond

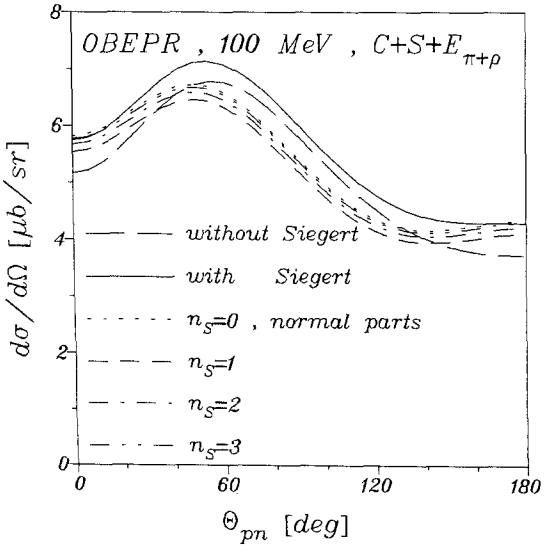

Fig. 2. Differential cross section at $q^{\text{lab}} = 100$ MeV for the OBEPR. The calculation is done with (solid) or without (long-dashed) use of ST. For the first case also the normal parts in the different gauges of (2.16) are shown

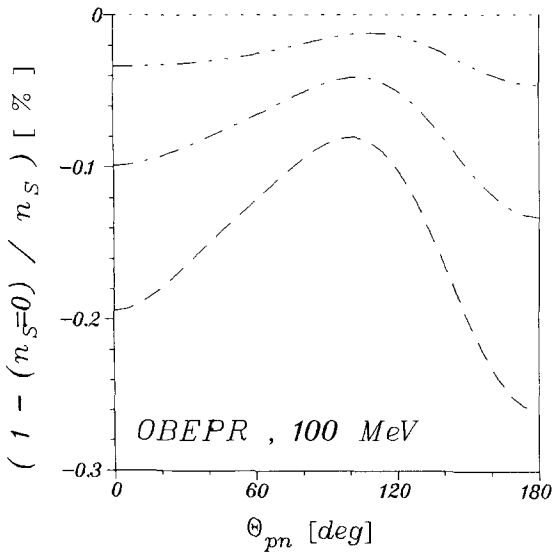

Fig. 3. Gauge dependence of the differential cross section at $q^{\text{lab}} = 100$ MeV for the OBEPR, if π- and ρ-MEC are included in $\hat{T}_b^{[L]}$. (Same notation of gauges as in Fig. 2)

π and ρ, which are implicitly included in the Siegert operator $\hat{T}_a^{[L]}$, contribute up to 10% in this case. The different normal parts form a narrow band with a width of about 5%, which reflects the gauge dependence and which, of course, is unacceptable for an accurate description of the cross section.

In comparison to the full curve of Fig. 2 one might be tempted to favour the z^L-gauge in contrast to the conclusions of ref. [12]. However, we do not consider such a conclusion as reasonable. First of all, it depends on the energy, which gauge gives the optimal approximation, if no MEC beyond the Siegert operators are considered. Secondly, what really counts are the results with additional explicit MEC. If these are consistent, all the different gauges give the same answer. Thus differences will occur only, if the MEC is not consistent with the potential. The gauge dependence introduced by this inconsistency in the small part $\hat{T}_b^{[L]}$ of $\hat{T}_{\text{el}}^{[L]}$ can be checked by changing the gauge.

In Fig. 3 we show the deviation from unity of the ratios of calculations with Siegert operators for $n_s = 0$ to $n_s = 0, \ldots, 3$. It is satisfying to see that the gauge dependence is less than 0.3% in the worst case even though the MEC is not completely consistent. This gives strong support to the neglect of other explicit currents beyond π- and ρ-MEC in $\hat{T}_b^{[L]}$. In this connection it is an interesting question to what extent the same argument holds for the ρ-MEC of Eq. (2.9), i.e., whether one has to include it or not. The answer is given in Fig. 4, where we show the deviation from unity of the ratios of the differential cross sections calculated with Siegert operators including only π-MEC in $\hat{T}_b^{[L]}$ to those including π- and ρ-MEC for the four gauges. The width of the resulting band, i.e. the gauge dependence, is qualitatively the same as in Fig. 3, whereas the absolute change in including ρ-MEC is significantly larger by an order of magnitude, but still very small compared to the ρ-contribution in the calculation with explicit currents only (Fig. 1 c), i.e., without Siegert theorem.

Thus, we may conclude that missing MEC or lack of consistency in our π- and ρ-currents will contribute at most on the 1%-level. This is in agreement with a model study using the Paris potential [13]. For OBEPQ and OBEPT the gauge depen-

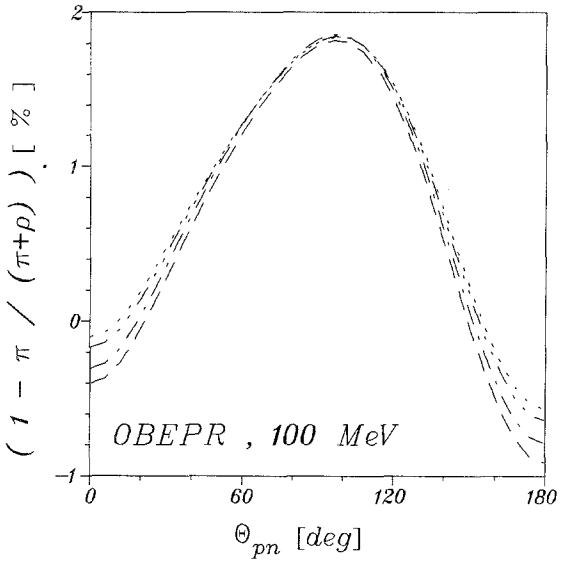

Fig. 4. The contribution of ρ-MEC in $\hat{T}_b^{[L]}$ for the cases considered in Fig. 3

dence is as weak as for the OBEPR, although formally the inconsistencies in the currents are stronger, due to the non-reduced relativistic meson-nucleon vertices.

The weak gauge dependence we found seems to contradict the recent results of Ying et al., see Fig. 3 of ref. [14]. For the OBEPR at $q^{\text{lab}} = 100$ MeV their forward differential cross section varies about 4% for the two gauges $n_s = 1$ and $n_s = 3$, whereas in our calculation this gauge dependence is less than 0.2%. In a forthcoming paper [15] these problems will be discussed in more detail.

We will now turn to the discussion of meson retardation effects in the electromagnetic interaction in connection with the OBEPT. For the OBEPs including non-retarded meson-propagators, i.e. OBEPQ and -R, current corrections referred to the static limit are of relative order p^2/m^2 at least. They originate only from relativistic corrections in the meson-nucleon vertices and we neglected them as discussed above. But for the time-dependent OBEPT a consistent construction of corresponding currents based on non-covariant perturbation theory yields corrections stemming from the energy dependence of the meson propagators, which are formally larger than the vertex-corrections, namely of relative order p^2/mm_α. In ref. [3] we presented in detail the formalism for constructing effective retarded current operators in N-space based on time-ordered perturbation theory in meson-nucleon Fock space. These currents involve the leading retardation corrections by expanding the retarded meson propagators in terms of p^2/mm_α, whereas p^2/m^2-corrections in these expansions as well as in the vertices were neglected. It was found that retardation effects in the π-MEC show up significantly even at low energies, and that they dominate the retardation effects in the wave functions in case of the Bryan-Scott-III potential.

In the present work we include retarded π- and ρ-MEC. For the pionic part only the retarded propagator functions of Eqs. (4.33) and (4.44) of ref. [3] have to be changed in order to be consistent with the corresponding OBEPT form factor of Eq. (2.4). The retarded ρ-MEC is restricted to its leading terms in g_ρ/f_ρ as in the static case, and it differs from the retarded π-MEC essentially only in the vertex structure. As in ref. [3] we pass over the problems concerning the non-orthogonality

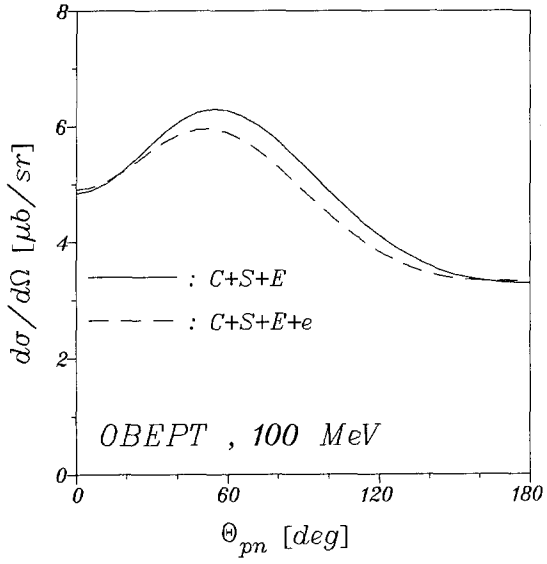

Fig. 5. Differential cross section at $q^{\text{lab}} = 100$ MeV for the OBEPT with (dashed) and without (solid) retardation corrections to the π- and ρ-MEC

of wave functions due to the explicit energy dependence of the OBEPT, since the dominant contributions seem to come from current retardation. But we take into account the presence of non-nucleonic components in the deuteron wave function by applying a normalization condition according to Eq. (D.14) of ref. [2]. We take the retardation parts of the π- and ρ-MEC as explicit current contributions, i.e. they are not calculated via corresponding retarded charge densities in the framework of ST.

In Fig. 5 the influence of current retardation on the differential cross section at $q^{\text{lab}} = 100$ MeV is shown. The tendency of lowering the maximum of the cross section found for the Bryan-Scott-III potential (see Fig. 10 of ref. [3]) is confirmed, but the effect of about 5% is less pronounced for OBEPT. If a theoretical accuracy of the order of 1% is needed, current retardation should be taken into account.

Besides the above-collected set of meson-exchange and non-relativistic one-body currents, we will further include the following three contributions:

(i) the relativistic spin-orbit (SO) current [4], which must be present in any comparison with real data;
(ii) isobar currents (IC) [1], which contribute non-negligibly even below π-threshold;
(iii) lowest-order relativistic corrections to the one-body currents [3].

All these contributions are taken as explicit currents, i.e. they are calculated without use of the ST. For the IC it is sufficient to take them in impulse approximation in the energy region considered. Whereas relativistic corrections in the meson-exchange currents are neglected systematically, the relativistic SO-current turned out to be very important. But this is no contradiction, since the relativistic SO-current represents a genuine off-shell effect [16], which would be present even for a purely local potential, i.e. without any exchange currents. The relativistic one-body current (see Eq. (4.18) of ref. [3]) partially includes the less important one-body part of the relativistic SO-current. To avoid double counting, this is taken into account, if both contributions are involved. Since the relativistic one-body

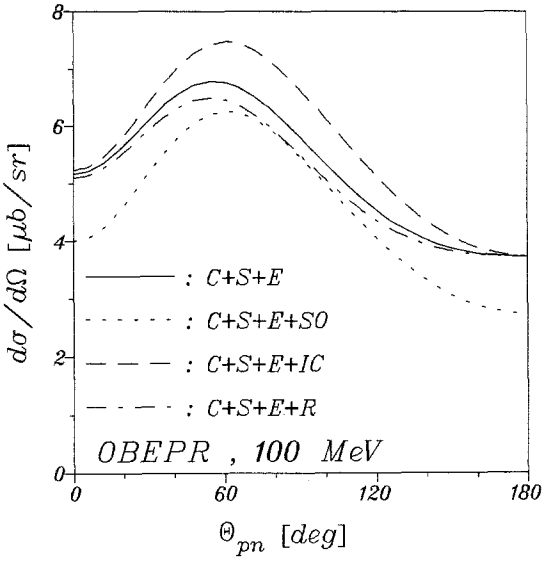

Fig. 6. Contributions of the relativistic spin-orbit current, isobar currents, and relativistic corrections to the one-body currents to the differential cross section at $q^{\text{lab}} = 100$ MeV for the OBEPR

current is frame-dependent, whereas corresponding relativistic corrections in the wave functions are neglected, the magnitude of its contribution will be a measure of this inconsistency.

A typical result is shown in Fig. 6 for the OBEPR at $q^{\text{lab}} = 100$ MeV. The classical part (solid line) is calculated without Siegert operators and is identical with that of Fig. 1 c (solid line). The relativistic SO-current decreases, whereas IC increase the cross section, the effects being maximal or minimal at extreme angles, respectively. Relativistic one-body currents turn out to be almost of the same order as current-retardation effects (Fig. 5). This important fact will be kept in mind for the judgement of significance of the retardation corrections.

3 Comparison with Experimental Data

In the following discussions of cross sections and polarization observables, the calculations for the different OBEPs always include, if not stated otherwise, as current contributions:

(i) static π- and ρ-MEC, calculated with the Siegert operator for the z^L-gauge,
(ii) isobar currents in the impulse approximation,
(iii) relativistic spin-orbit current,
(iv) lowest p^2/m^2-order corrections to the one-body currents.

In case of the retarded OBEPT, additionally included are

(v) lowest $p^2/mm_{(\pi,\rho)}$-order retardation corrections to the π- and ρ-MEC.

Fig. 7 shows the total cross section for deuteron photodisintegration with the different OBE-models in comparison with experimental data. For low energies (Fig. 7 a) the theoretical results are very similar, but even the simple Bethe-Peierls formula [17] would give an equally good description of the experiments in that energy region [1]. For higher energies (Fig. 7 b), however, the cross section for the

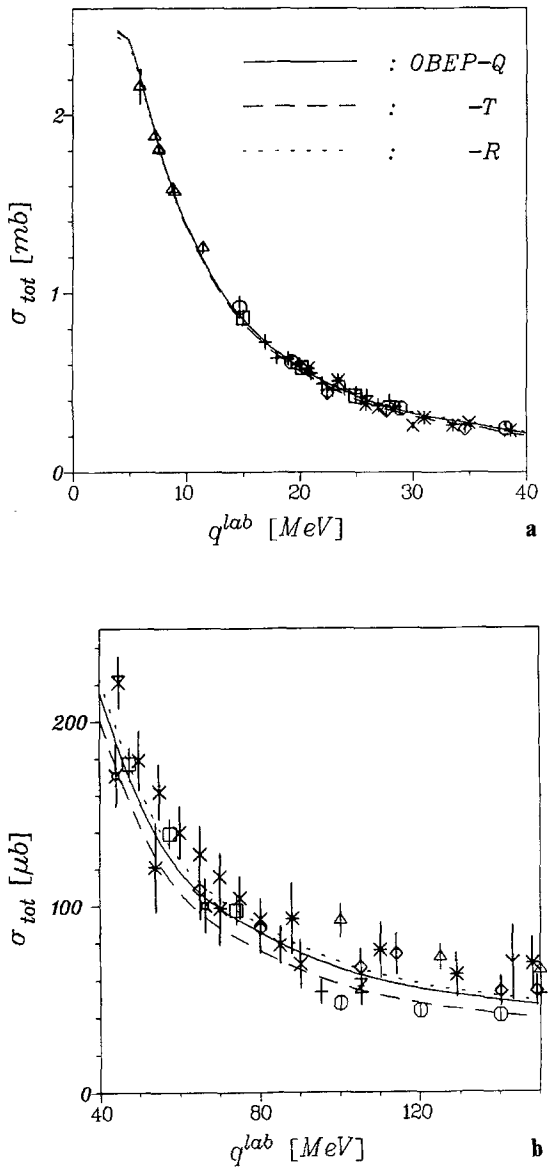

Fig. 7. Total cross section for the different OBE models. Data points in Fig. 7 a: [23]: □, [24]: ○, [25]: △, [26]: +, [27]: ×, [28]: ◇, [29]: ∗, and in Fig. 7 b: [24]: □, [30]: ○, [31]: △, [32]: +, [33]: ×, [34]: ◇, [35]: ∗, [27] ⧖, [36]: Z, [37]: Y and [28]: ⧓

OBEPT lies distinctly below the cross sections for the two unretarded models. This effect is due to current retardation of π- and ρ-exchange. It is not caused by the renormalization of the deuteron wave function (Eq. (D.14) of ref. [2]) which we have used for the energy-dependent OBEPT, because it leads to an energy-independent renormalization of the cross section by about 3%, and therefore is already present at low energies (Fig. 7 a). With respect to the experimental data, the situation is not very clear for the higher energies: Up to 100 MeV the predictions of all the different OBE models are compatible with experiment, but above 100 MeV the OBEPT model seems to systematically underestimate the total cross section.

The differential cross sections at laboratory photon energies of 60, 100, and 140 MeV are shown in Figs. 8 a–c. Concerning the different OBE models the OBEPQ curves always lie slightly below the OBEPR calculations, and the difference

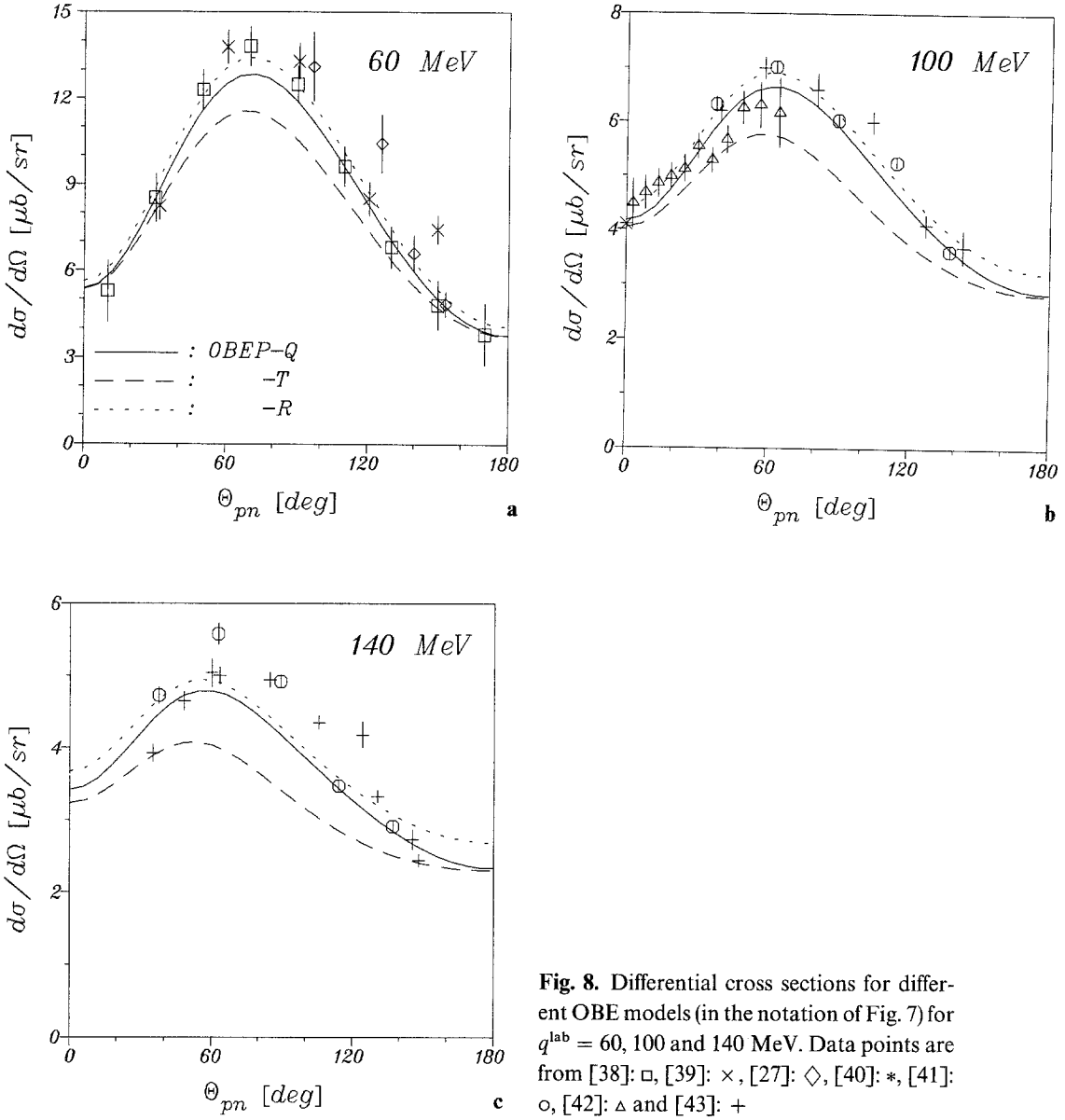

Fig. 8. Differential cross sections for different OBE models (in the notation of Fig. 7) for $q^{lab} = 60$, 100 and 140 MeV. Data points are from [38]: □, [39]: ×, [27]: ◇, [40]: *, [41]: o, [42]: △ and [43]: +

increases for extreme (forward and backward) angles with higher energies. The retarded OBEPT model, however, gives distinct lower cross sections compared to the unretarded potentials. Especially the maxima of the angular distributions are strongly reduced, whereas the values under extreme angles are less affected.

At 60 MeV the experimental data are well described in the maximum region by the unretarded potentials, whereas at extreme angles any of the models agrees well with the data. Also at 100 MeV the OBEPQ or -R calculations are compatible with the experimental values over the whole angular range, while the OBEPT calculation lies too low. At 140 MeV the experimental situation is not very satisfactory, because different experiments are still not consistent with each other. But qualitatively, the

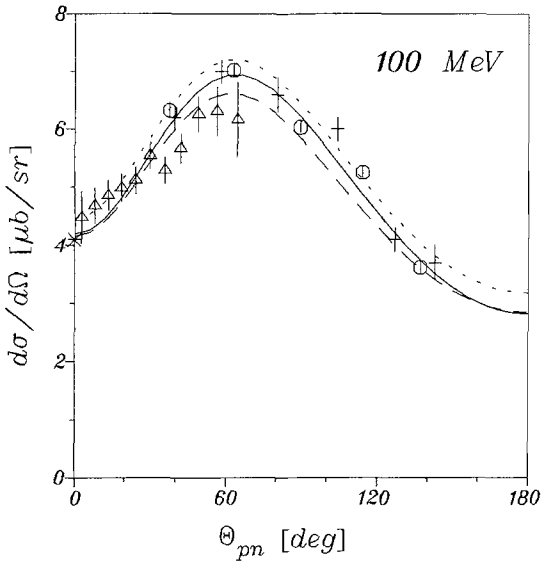

Fig. 9. As Fig. 8 but without retarded MEC contributions in the case of the OBEPT and without relativistic corrections to the one-body currents in case of all three OBEPs

theoretical cross sections for the unretarded potentials agree considerably better with experiment than for the retarded one. On the other hand two-body isobar currents are missing which are known to become more important [18].

In Fig. 9 the retardation corrections to the exchange currents in the OBEPT case and the relativistic one-body currents for all these OBE models are switched off. Both corrections lower the cross sections. Without retarded currents the OBEPT calculation seems to be in better agreement with the experimental data. But this cannot be a valid argument against the inclusion of retardation effects, because they are needed for consistency within the non-covariant formalism underlying the OBEPT model. On the contrary, since the retardation effects turns out to be so important, while the agreement with experiments is worsened, it is an indication that, if the underlying physical ideas are acceptable, the restriction to the lowest order, i.e. p^2/mm_α, is not sufficient. Since the next order in the expansion of the retarded propagators appearing in the exchange currents, i.e. p^2/m^2, is a genuine relativistic one, its inclusion would require a complete relativistic calculation up to this order.

We will now consider the energy dependence of the differential cross section at forward and backward angles (Figs. 10a, b). It is well known that the originally puzzling discrepancy between experimental data and theoretical calculations at forward angles was essentially resolved by including the relativistic spin-orbit current [4, 16, 19]. The low D-state probabilities of the Bonn OBEPs in addition lower the cross section at the forward direction. The differences within the different OBE calculations are quite small and the results are rather insensitive to the inclusion of retardation corrections to the MEC or to relativistic corrections to the one-body currents.

The recent experimental data from ref. [46] fit quite well into the theoretical predictions for forward as well as for backward angles. The same is true for the recent data of ref. [44], except the 14.7 MeV measurement at 0° which gives two high a value. In the energy region between 20 and 50 MeV there are still some data points

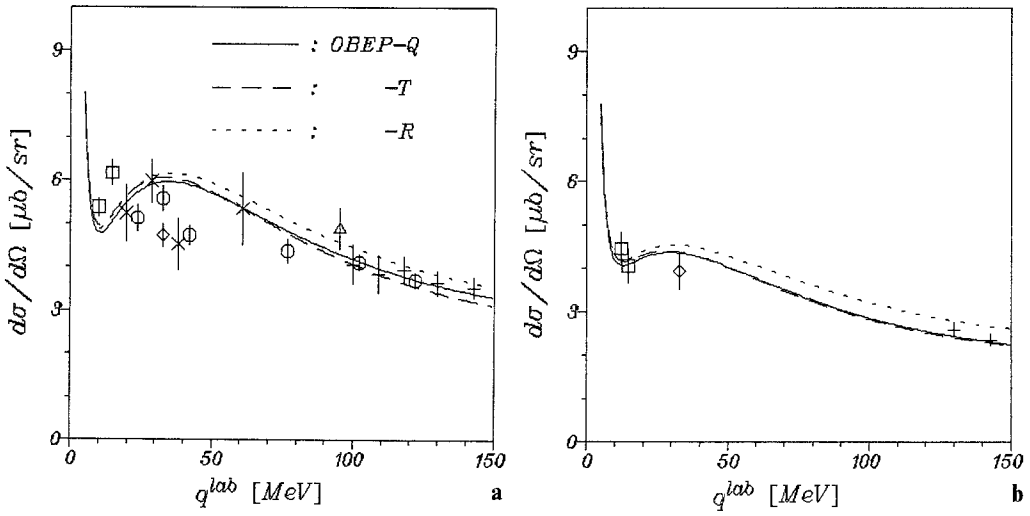

Fig. 10. Differential cross sections at forward (**a**) and backward (**b**) angles for the different OBE models. Data points are from [44]: □, [40]: ○, [45], △, [46]: +, [47]: × and [48]: ◇

distinctly below the theoretical curves for the forward cross section, but experimental effort is under way for remeasuring the cross section in this energy region. At 180° more data is certainly needed.

In the unpolarized cross section, as considered so far, most of the detailed information originally present in the theoretical calculated T-matrix is lost by averaging and summing over spin degrees of freedom. In principle, any set of 23 independent polarization observables would carry the whole information included in the T-matrix [20]. Although one is presently still far away from the possibility of measuring such a set of observables, which is still not yet defined explicitly, polarization observables are receiving increasing interest, as the continuous beam accelerator techniques and development of polarized targets and polarimeters proceed further.

Up to now only a few polarization observables for deuteron photodisintegration have been measured, for instance, the photon-asymmetry Σ^l and the polarization of the outgoing neutron $P_y(n)$, for which we show our theoretical results in Fig. 11 and Fig. 12, respectively. In case of the photon-asymmetry it is interesting to see that the OBEPT model, including retarded MEC, improves the description of the experimental data.

The neutron polarization, however, turns out to be very insensitive to the OBE versions used. In addition, $P_y(n)$ is also insensitive to the retardation corrections in the current, while for Σ^l the OBEPT curves would move significantly towards the curves for the unretarded models, if the retardation corrections to the MEC would be switched off.

Besides the observables discussed so far, we have calculated all 288 polarization observables defined in ref. [20] and have looked systematically for possible candidates which would allow to differentiate between different OBEPs. Most of the observables differ with respect to the different OBEPs in absolute size by less than 0.05 at $q^{\text{lab}} = 100$ MeV for example. Therefore, the different OBE models can

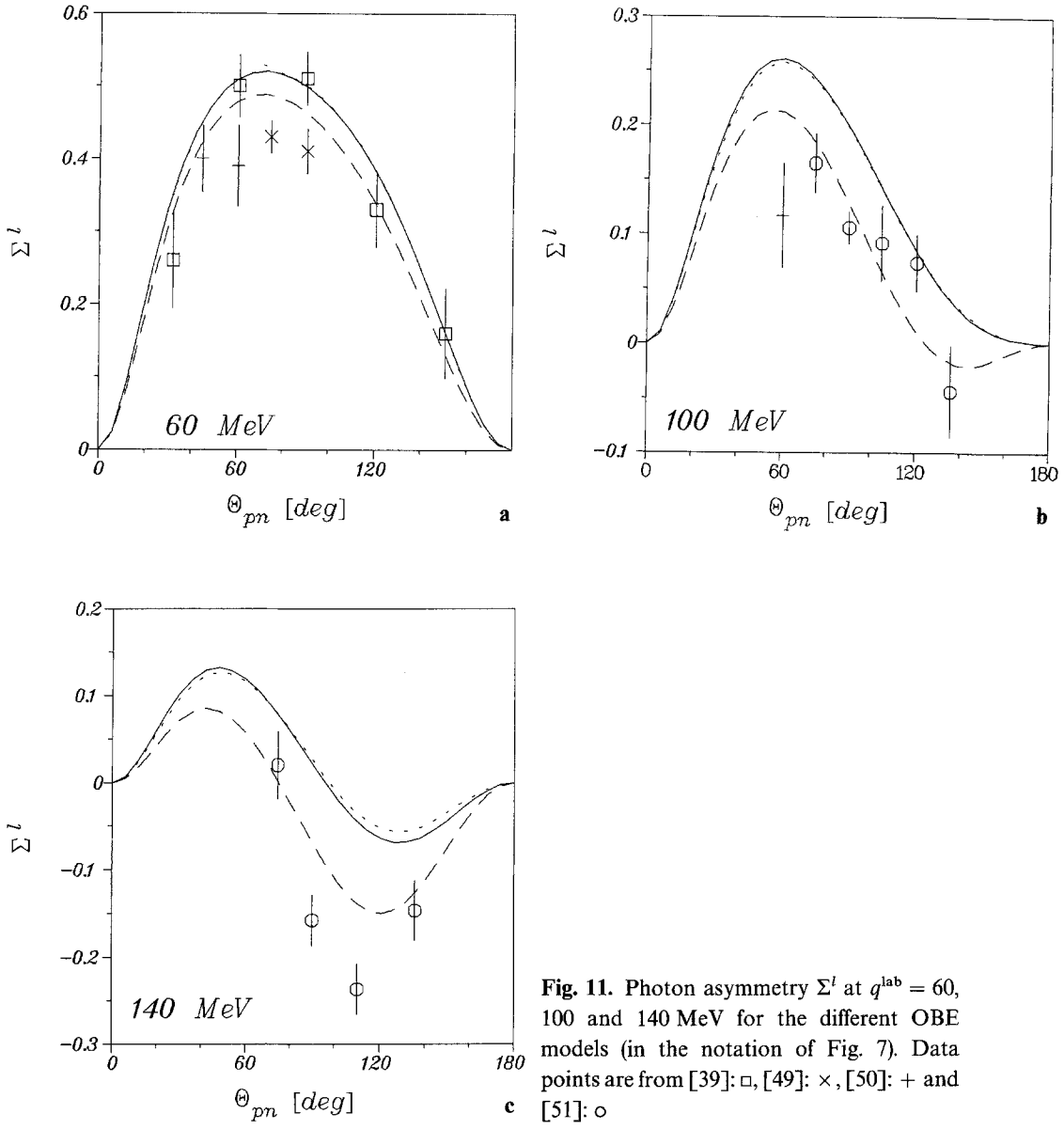

Fig. 11. Photon asymmetry Σ^l at $q^{\text{lab}} = 60$, 100 and 140 MeV for the different OBE models (in the notation of Fig. 7). Data points are from [39]: □, [49]: ×, [50]: + and [51]: o

introduce large relative differences only in observables which are small in absolute magnitude. In general, the results for the OBEPQ and OBEPR are more similar to each other than compared to the OBEPT predictions. But there are a number of observables with considerable different angular distributions for all three models, and hence they could serve to differentiate between different models in the future experiments. As an illustration we show in Fig. 13 the following observables at $q^{\text{lab}} = 100$ MeV:

— T_{22}^c: a tensor target asymmetry with circularly polarized photons;
— $P_z^{22}(p)$: a tensor target asymmetry of the proton polarization along the z-axis (the direction of the outgoing proton momentum in the c.m. system);

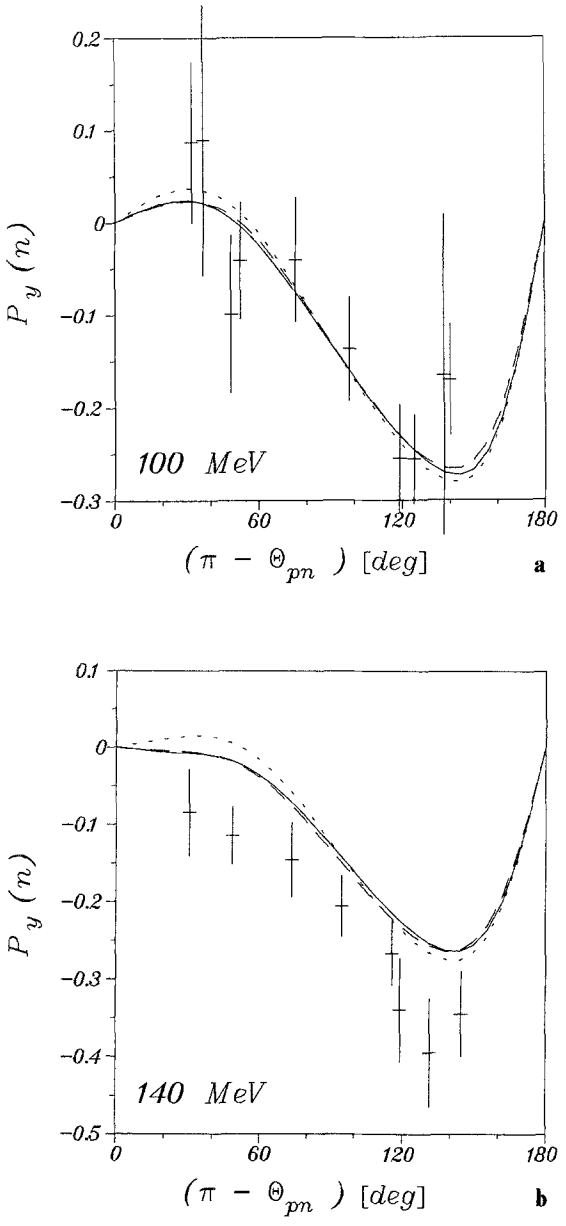

Fig. 12. Neutron polarization $P_y(n)$ at $q^{\text{lab}} =$ 100 and 140 MeV for the different OBE models (in the notation of Fig. 7). Data points are from [43]

— $P_z^{c,11}(p)$ and $P_z^{c,11}(n)$: a vector target asymmetry with circularly polarized photons of the proton or neutron polarization along the z-axis, respectively;
— $P_{yy}^{l,10}$: a vector target asymmetry with linearly polarized photons of the y-components (perpendicular to the c.m. reaction plane) of proton and neutron double polarization;
— $P_{xy}^{l,11}$: as $P_{yy}^{l,10}$ but with x-component of the proton polarization and for a different vector target asymmetry.

Note that (T_{22}^c and $P_z^{22}(p)$) are two-, $P_z^{c,11}(p/n)$ three- and ($P_{yy}^{l,10}$ and $P_{xy}^{l,11}$) four-fold polarization observables. The partially dramatic dependence on the underlying OBE model underlines the rich information contained in polarization observables

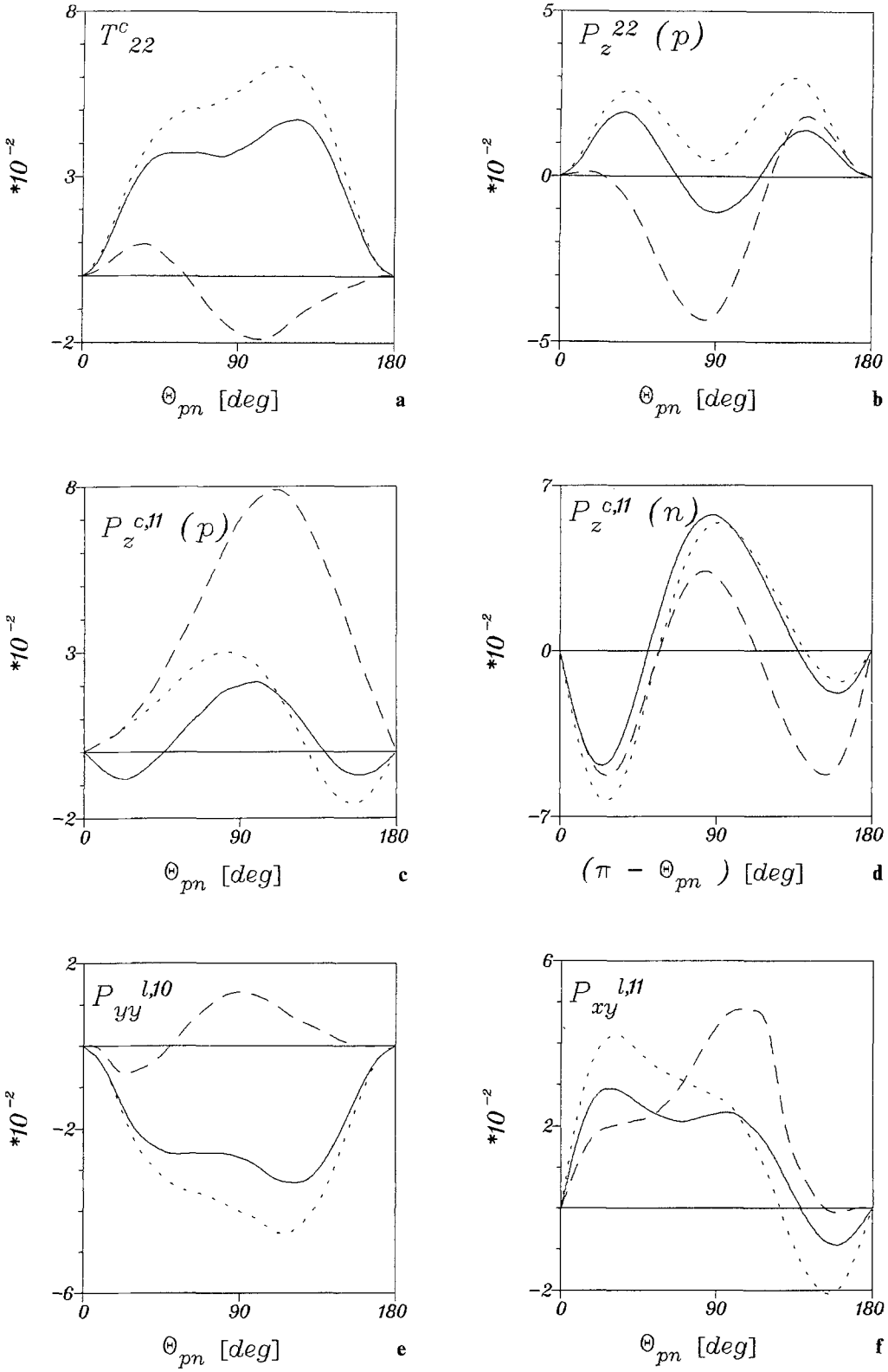

Fig. 13. Selected examples of polarization observables for the different OBE models at $q^{\text{lab}} = 100$ MeV (in the notation of Fig. 7)

still to be measured in deuteron photodisintegration. A systematic discussion of all polarization observables will be presented elsewhere.

4 Summary

We have studied deuteron photodisintegration below π-threshold using the OBE approximations OBEPQ, -T and -R to the recent Bonn potential. Consistent static meson-exchange currents for the non-relativistic π- and the dominant ρ-part of the OBEPs are included as explicit currents. In case of the time-dependent OBEPT also the leading retardation corrections to the π- and ρ-MEC are constructed and taken into account. Missing static currents beyond these π- and ρ-currents are incorporated via the Siegert theorem up to a very high degree. The results show almost no dependence on the electromagnetic gauge for the Siegert operators. In addition, also the relativistic spin-orbit current and one-body isobar currents are included in our calculation.

The retardation effects in the electromagnetic currents turn out to be much less pronounced in the unpolarized cross section than in a former model study using the BS-III potential. However, one should be cautioned to generalize this result because uncertainties arise from non-negligible higher-order corrections, which are of genuine relativistic order and cannot be calculated consistently within a non-relativistic framework.

All unpolarized data on deuteron photodisintegration below π-threshold, i.e., total and differential cross sections especially at forward and backward angles, can be satisfactorily described by the OBEPQ or -R, within the existing experimental uncertainties. On the other hand, the OBEPT underestimates slightly the maximum of the differential cross section. Polarization observables provide additional tests for present theoretical models of the electromagnetic structure implicitly contained in the nuclear force model. Their accurate knowledge is indispensable for a better theoretical understanding. For example, retardation effects in the electromagnetic interaction show up significantly in the photon asymmetry at 100 MeV. Also certain, not yet measured observables differentiate significantly between different OBE models.

In conclusion we may state that the OBE approximations to the Bonn "full model" provide a satisfactory description of deuteron photodisintegration and thus may be used for photonuclear reactions in general.

Appendix. OBE Expressions in $(ls)j$-Basis

For the sake of applicability we summarize here the explicit partial-wave matrix elements of the potential

$$V(p, p'; jsll') = \int d\Omega_{\vec{p}} \int d\Omega_{\vec{p}'} \langle (ls)jm|\hat{p}\rangle \langle \vec{p}|\hat{V}|\vec{p}'\rangle \langle \hat{p}'|(l's)jm\rangle \tag{A.1}$$

($p = |\vec{p}|$, $\hat{p} = \vec{p}/p$) for the different OBEPs in $(ls)j$-basis as required for solving the wave equations (2.37), (2.39) of ref. [3] in momentum space for the N-N scattering states and the deuteron.

We first consider the QBEPQ. Taking the corresponding potential amplitudes (E.21)–(E.23) of ref. [2] and passing through the algebra of (A.1) one finally obtains for pseudo-scalar, scalar and vector mesons:

$$V_{ps}(p,p';jsll') = -g_{ps}^2 \frac{1}{m\sqrt{\varepsilon_p\varepsilon_{p'}}} \frac{3}{8\pi^2}(-)^{j+s}\hat{l}\hat{l}'\hat{s}^2 * \Big\{ C(jsll')(p^2\Omega^2(p',p)a_{l'}(p',p)$$
$$+ (p \leftrightarrow p', l \leftrightarrow l')) + 2pp' \sum_L D(jsll'L)a_L(p,p') \Big\}, \tag{A.2}$$

$$V_s(p,p';jsll') = -g_s^2 \frac{1}{m\sqrt{\varepsilon_p\varepsilon_{p'}}} \frac{1}{16\pi^2} * \Big\{ \overline{\varepsilon}_p\overline{\varepsilon}_{p'}\delta_{ll'}a_l(p,p') - 2pp'\delta_{ll'}\sum_L B(lL)a_L(p,p')$$
$$+ 12pp'\delta_{ll'}\delta_{s1}(-)^{j+l}\hat{l}^2 \begin{Bmatrix} 1 & l & l \\ j & 1 & 1 \end{Bmatrix} \sum_L F(lL)a_L(p,p')$$
$$+ 36\frac{p^2p'^2}{\overline{\varepsilon}_p\overline{\varepsilon}_{p'}}(-)^{l+s+j}\hat{l}\hat{l}'\hat{s}^2 \sum_L G(jsll'L)a_L(p,p') \Big\}, \tag{A.3}$$

$$V_v(p,p';jsll') = \frac{1}{m\sqrt{\varepsilon_p\varepsilon_{p'}}} \frac{1}{16\pi^2}$$
$$* \Big\{ \overline{\varepsilon}_p\overline{\varepsilon}_{p'}\delta_{ll'} \Big[(g_v+f_v)^2 - 2(g_v+f_v)\frac{f_v}{m}(\varepsilon_{p'}+\varepsilon_p - m) + \frac{f_v^2}{2m^2}(3\varepsilon_{p'}\varepsilon_p - m^2) \Big] a_l(p,p')$$
$$+ \overline{\varepsilon}_p\overline{\varepsilon}_{p'}pp'\delta_{ll'}\frac{f_v^2}{2m^2}\sum_L B(lL)a_L(p,p')$$
$$+ pp'\delta_{ll'} \Big[6(g_v+f_v)^2 - 4(g_v+f_v)f_v - \frac{f_v^2}{m^2}(3\varepsilon_{p'}\varepsilon_p - m^2 + (\varepsilon_{p'}-\varepsilon_p)^2) \Big]$$
$$* \Big(\sum_L B(lL)a_L(p,p') - \delta_{s1}(-)^{j+l}6\hat{l}^2 \begin{Bmatrix} 1 & l & l \\ j & 1 & 1 \end{Bmatrix} \sum_L F(lL)a_L(p,p') \Big)$$
$$+ \frac{p^2p'^2}{\overline{\varepsilon}_p\overline{\varepsilon}_{p'}} \Big[(g_v+f_v)^2 + 2(g_v+f_v)\frac{f_v}{m}(\varepsilon_{p'}+\varepsilon_p+m) + \frac{f_v^2}{2m^2}(3\varepsilon_{p'}\varepsilon_p - m^2) \Big]$$
$$* 36(-)^{l+s+j}\hat{s}^2\hat{l}\hat{l}' \sum_L G(jsll'L)a_L(p,p')$$
$$- p^2p'^2\frac{f_v^2}{m^2} \Big(\delta_{ll'}\sum_L H(lL)a_L(p,p') + \delta_{s1}(-)^j 6\hat{l}\hat{l}' \begin{Bmatrix} j & 1 & l \\ 1 & l' & 1 \end{Bmatrix} \sum_L K(ll'L)a_L(p,p') \Big)$$
$$+ \frac{p^3p'^3}{\overline{\varepsilon}_p\overline{\varepsilon}_{p'}}\frac{f_v^2}{m^2}(-)^{l+s+j}18\hat{s}^2\hat{l}\hat{l}' \sum_L Q(jsll'L)a_L(p,p') - (-)^j 18\hat{l}\hat{l}'C(jsll'L)$$
$$* \Big[p'^2\Omega^2(p,p') \Big((g_v+f_v)^2 - \frac{f_v}{2m}(\varepsilon_p - \varepsilon_{p'}) \Big)^2 a_l(p,p') + (p \leftrightarrow p', l \leftrightarrow l') \Big]$$
$$- pp' \Big[(g_v+f_v)^2 - \frac{f_v^2}{4m^2}(\varepsilon_{p'}-\varepsilon_p)^2 \Big] (-)^j 36\hat{l}\hat{l}' \sum_L D(jsll'L)a_L(p,p') \Big\}, \tag{A.4}$$

with

$$C(jsll') = \sum_J \hat{J}^2 \begin{pmatrix} 1 & 1 & J \\ 0 & 0 & 0 \end{pmatrix} \begin{pmatrix} l & l' & J \\ 0 & 0 & 0 \end{pmatrix} \begin{Bmatrix} s & l' & j \\ l & s & J \end{Bmatrix} \begin{Bmatrix} \frac{1}{2} & \frac{1}{2} & s \\ \frac{1}{2} & \frac{1}{2} & s \\ 1 & 1 & J \end{Bmatrix}, \tag{A.5}$$

$$D(jsll'L) = (-)^{L+1}L^2 \begin{pmatrix} L & l & 1 \\ 0 & 0 & 0 \end{pmatrix} \begin{pmatrix} L & l' & 1 \\ 0 & 0 & 0 \end{pmatrix} \sum_J \hat{J}^2 \begin{Bmatrix} s & l' & j \\ l & s & J \end{Bmatrix} \begin{Bmatrix} l' & 1 & L \\ 1 & l & J \end{Bmatrix} \begin{Bmatrix} \frac{1}{2} & \frac{1}{2} & s \\ \frac{1}{2} & \frac{1}{2} & s \\ 1 & 1 & J \end{Bmatrix}, \tag{A.6}$$

$$B(lL) = \hat{L}^2 \begin{pmatrix} l & 1 & L \\ 0 & 0 & 0 \end{pmatrix}^2, \tag{A.7}$$

$$F(lL) = B(lL)\begin{Bmatrix} 1 & l & l \\ L & 1 & 1 \end{Bmatrix}, \tag{A.8}$$

$$\begin{aligned} G(jsll'L) = \hat{L}^2 \sum_{J\alpha\beta J_1 J_2} \hat{J}^2 \begin{Bmatrix} s & l' & j \\ l & s & J \end{Bmatrix} \hat{\alpha}^2 \hat{\beta}^2 \begin{pmatrix} 1 & 1 & \alpha \\ 0 & 0 & 0 \end{pmatrix} \begin{pmatrix} 1 & 1 & \beta \\ 0 & 0 & 0 \end{pmatrix} \\ * \begin{pmatrix} l & L & \alpha \\ 0 & 0 & 0 \end{pmatrix} \begin{pmatrix} l' & L & \beta \\ 0 & 0 & 0 \end{pmatrix} \begin{Bmatrix} l' & l & J \\ \alpha & \beta & L \end{Bmatrix} (-)^{J_1+J_2} \hat{J}_1^2 \hat{J}_2^2 \\ * \begin{Bmatrix} 1 & 1 & J_1 \\ \frac{1}{2} & \frac{1}{2} & \frac{1}{2} \end{Bmatrix} \begin{Bmatrix} 1 & 1 & J_2 \\ \frac{1}{2} & \frac{1}{2} & \frac{1}{2} \end{Bmatrix} \begin{Bmatrix} \frac{1}{2} & \frac{1}{2} & s \\ \frac{1}{2} & \frac{1}{2} & s \\ J_1 & J_2 & J \end{Bmatrix} \begin{Bmatrix} 1 & 1 & \alpha \\ 1 & 1 & \beta \\ J_1 & J_2 & J \end{Bmatrix}, \end{aligned} \tag{A.9}$$

$$H(lL) = \hat{L}^2 \sum_J \hat{J}^2 \begin{pmatrix} 1 & 1 & J \\ 0 & 0 & 0 \end{pmatrix}^2 \begin{pmatrix} l & L & J \\ 0 & 0 & 0 \end{pmatrix}^2, \tag{A.10}$$

$$\begin{aligned} K(ll'L) = (-)^L \hat{L}^2 \sum_{\alpha\beta} \hat{\alpha}^2 \hat{\beta}^2 \begin{pmatrix} 1 & 1 & \alpha \\ 0 & 0 & 0 \end{pmatrix} \begin{pmatrix} 1 & 1 & \beta \\ 0 & 0 & 0 \end{pmatrix} \begin{pmatrix} l & L & \alpha \\ 0 & 0 & 0 \end{pmatrix} \begin{pmatrix} l' & L & \beta \\ 0 & 0 & 0 \end{pmatrix} \\ * \begin{Bmatrix} \beta & \alpha & 1 \\ 1 & 1 & 1 \end{Bmatrix} \begin{Bmatrix} l' & l & 1 \\ \alpha & \beta & L \end{Bmatrix}, \end{aligned} \tag{A.11}$$

$$\begin{aligned} Q(jsll'L) = \hat{L}^2 \sum_{J\alpha\beta\mathscr{L}\mathscr{L}'J_1J_2} (-)^J \hat{J}^2 \begin{Bmatrix} s & l' & j \\ l & s & J \end{Bmatrix} \hat{\alpha}^2 \hat{\beta}^2 \begin{pmatrix} 1 & 1 & \alpha \\ 0 & 0 & 0 \end{pmatrix} \begin{pmatrix} 1 & 1 & \beta \\ 0 & 0 & 0 \end{pmatrix} \\ * \hat{\mathscr{L}}^2 \hat{\mathscr{L}}'^2 \begin{pmatrix} 1 & \alpha & \mathscr{L} \\ 0 & 0 & 0 \end{pmatrix} \begin{pmatrix} 1 & \beta & \mathscr{L}' \\ 0 & 0 & 0 \end{pmatrix} \begin{pmatrix} l & L & \mathscr{L} \\ 0 & 0 & 0 \end{pmatrix} \begin{pmatrix} l' & L & \mathscr{L}' \\ 0 & 0 & 0 \end{pmatrix} \\ * \begin{Bmatrix} \mathscr{L}' & \mathscr{L} & J \\ \alpha & \beta & 1 \end{Bmatrix} \begin{Bmatrix} l' & l & J \\ \mathscr{L} & \mathscr{L}' & L \end{Bmatrix} \\ * (-)^{J_1+J_2} \hat{J}_1^2 \hat{J}_2^2 \begin{Bmatrix} 1 & 1 & J_1 \\ \frac{1}{2} & \frac{1}{2} & \frac{1}{2} \end{Bmatrix} \begin{Bmatrix} 1 & 1 & J_2 \\ \frac{1}{2} & \frac{1}{2} & \frac{1}{2} \end{Bmatrix} \begin{Bmatrix} \frac{1}{2} & \frac{1}{2} & s \\ \frac{1}{2} & \frac{1}{2} & s \\ J_1 & J_2 & J \end{Bmatrix} \begin{Bmatrix} 1 & 1 & \alpha \\ 1 & 1 & \beta \\ J_1 & J_2 & J \end{Bmatrix} \end{aligned} \tag{A.12}$$

and

$$\varepsilon_p = \sqrt{p^2 + m^2}, \qquad \bar{\varepsilon}_p = \varepsilon_p + m, \qquad \Omega^2(p, p') = \bar{\varepsilon}_p / \bar{\varepsilon}_{p'}. \tag{A.13}$$

For isovector mesons a factor $\vec{\tau}_1 \cdot \vec{\tau}_2$ has to be included in the expressions (A.2)–(A.4). The coefficients a_L are defined via an angular decomposition of the product of strong form factors times static meson propagators

$$\frac{F^2((\vec{p}' - \vec{p})^2)}{\omega^2_{\vec{p}'-\vec{p}}} = 2\pi \sum_{LM} \langle \hat{p} | LM \rangle a_L(p, p') \langle LM | \hat{p}' \rangle, \tag{A.14}$$

which yields

$$a_L(p, p') = (\Lambda_\alpha^2 - m_\alpha^2)^{2n_\alpha} \int_{-1}^{1} dz\, P_L(z) \tilde{\omega}^{-2}(p, p', z, m_\alpha) \tilde{\omega}^{-4}(p, p', z, \Lambda_\alpha), \tag{A.15}$$

with

$$\tilde{\omega}(p, p', z, m_\alpha) = (p^2 + p'^2 - 2pp'z + m_\alpha^2)^{1/2}, \tag{A.16}$$

for any of the mesons considered with masses m_α, cut-off parameters Λ_α and regularization orders $2n_\alpha$. Note that we have not used an approximation like (E.49) of ref. [2] for the left-hand side of (A.14). In the static case the a_L coefficients may be expressed by Legendre polynomials of the second kind according to

$$a_L(p, p') = \frac{1}{pp'}\left\{Q_L(x(m_\alpha)) - \sum_{k=0}^{2n_\alpha-1} \frac{(-)^k}{k!}(x(\Lambda_\alpha) - x(m_\alpha))^k \frac{d^k}{dx^k(\Lambda_\alpha)} Q_L(x(\Lambda_\alpha))\right\}, \tag{A.17}$$

where

$$x(m_\alpha) = \frac{1}{2pp'}(p^2 + p'^2 + m_\alpha^2), \tag{A.18}$$

and calculated analytically.

For the OBEPT the partial-wave amplitudes of (A.2)–(A.4) have to be changed threefold:

(i) Due to the fact that the OBEPT is not to be understood in connection with the BbS-equation, no factors of minimal relativity appear, i.e. the amplitudes have to be multiplied by

$$\frac{m}{\sqrt{\varepsilon_p \varepsilon_{p'}}}.$$

(ii) Because the off-shell term

$$(\varepsilon_{p'} - \varepsilon_p)(g_{0\mu} - \gamma_\mu \gamma_0)$$

for the ρ-meson is dropped in time-ordered perturbation theory the underlined terms in (A.4) have to be absent for the OBEPT and the terms underlined by dashed lines have to be substituted by

$$\varepsilon_p^2 + \varepsilon_{p'}^2 + \varepsilon_p \varepsilon_{p'} - m^2.$$

(iii) Retardation of the meson propagators changes the a_L coefficients: The $\tilde{\omega}^{-2}$-term of the right-hand side of (A.15) has to be substituted by

$$\tilde{\omega}^{-1}(p, p', z, m_\alpha)[\tilde{\omega}(p, p', z, m_\alpha) + (\varepsilon_p + \varepsilon_{p'} - 2m) - E]^{-1}$$

and the resulting retarded a_L-coefficients have to be calculated by numerical integration. Here, E denotes the starting energy of the LS-type wave equation.

Finally, the partial-wave amplitudes for the OBEPR can be obtained from the corresponding amplitudes of the static BS-III potential given in ref. [21] by including the factor of minimal relativity, i.e., by multiplying them with $\sqrt{\varepsilon_{p'}\varepsilon_p}/m$ and taking the resulting amplitudes up to order p^2/m^2. Again, we have not used the approximation (F.9) of ref. [2].

References

1. Arenhövel, H.: In: Proceedings of International School of Intermediate-Energy Nuclear Physics, Verona (Bergère, R., Costa, S., Schaerf, C., eds.), p. 55. Singapore: World Scientific 1986
2. Machleidt, R., Holinde, K., Elster, Ch.: Phys. Rep. **149**, 1 (1987)
3. Schmitt, K.-M., Arenhövel, H.: Few-Body Systems **6**, 117 (1989)
4. Cambi, A., Mosconi, B., Ricci, P.: Phys. Rev. Lett. **48**, 462 (1982)
5. Blankenbecler, R., Sugar, R.: Phys. Rev. **142**, 1051 (1966)
6. Salpeter, E. E., Bethe, H. A.: Phys. Rev. **84**, 1232 (1951)
7. Bryan, R., Scott, B. L.: Phys. Rev. **177**, 1435 (1969)
8. Schmitt, K.-M., Arenhövel, H.: Preprint MKPH-T-87-5. Mainz: Institut für Kernphysik 1987
9. Fabian, W., Arenhövel, H.: Nucl. Phys. **A258**, 461 (1976)
10. Arenhövel, H.: Z. Phys. **A302**, 25 (1981)
11. Partovi, F.: Ann. Phys. **27**, 79 (1964)
12. Friar, J. L., Fallieros, S.: Phys. Rev. **C29**, 1645 (1984)
13. Buchmann, A., Leidemann, W., Arenhövel, H.: Nucl. Phys. **A443**, 726 (1985)
14. Ying, S., Henley, E. M., Miller, G. A.: Phys. Rev. **C38**, 1584 (1988)
15. Schmitt, K.-M., et al.: (to be published)

16. Wilhelm, P., Leidemann, W., Arenhövel, H.: Few-Body Systems **3**, 111 (1988)
17. Bethe, H. A., Peierls, R.: Proc. Roy. Soc. **A148**, 146 (1935)
18. Leidemann, W., Arenhövel, H.: Nucl. Phys. **A465**, 573 (1987)
19. Friar, J. L., Gibson, B. F., Payne, G. L.: Phys. Rev. **C30**, 441 (1984)
20. Arenhövel, H.: Few-Body Systems **4**, 55 (1988)
21. Schmitt, K.-M.: Doctoral Thesis. Mainz University 1986
22. Fabian, W., Arenhövel, H.: Nucl. Phys. **A314**, 253 (1979)
23. Ahrens, J., et al.: Phys. Lett. **52B**, 49 (1974)
24. Bernabei, R., et al.: Phys. Rev. Lett. **57**, 1542 (1986)
25. Birenbaum, Y., Kahane, S., Moreh, R.: Phys. Rev. **C32**, 1825 (1985)
26. Skopik, D. M., et al.: Phys. Rev. **C9**, 531 (1974)
27. Weissman, B., Schultz, H. L.: Nucl. Phys. **A174**, 129 (1971)
28. Allen, L.: Phys. Rev. **98**, 705 (1955)
29. Bosman, M., et al.: Phys. Lett. **82B**, 212 (1979)
30. Kose, R., et al.: Z. Phys. **202**, 364 (1967)
31. Dougan, P., Ramsay, V., Stiefler, W.: Z. Phys. **A280**, 341 (1977)
32. Smith, A. M., et al.: J. Phys. (Proc. Phys. Soc.), Ser. 2A **1**, 553 (1968)
33. Galey, J. A.: Phys. Rev. **117**, 763 (1960)
34. Whalin, E. A., et al.: Phys. Rev. **101**, 377 (1956)
35. Alexandrov, Iu. A., et al.: JETP **33**, 614 (1957)
36. Keck, J. C., Tollestrup, A. V.: Phys. Rev. **101**, 360 (1956)
37. Dixon, D. R., Bandtel, K. C.: Phys. Rev. **104**, 1730 (1956)
38. De Pascale, M. P., et al.: Phys. Lett. **119B**, 30 (1982)
39. De Pascale, M. P., et al.: Phys. Rev. **C32**, 1830 (1985)
40. Hughes, R. J., et al.: Nucl. Phys. **A267**, 329 (1976)
41. De Sanctis, E., et al.: Phys. Rev. **C34**, 413 (1986)
42. Meyer, H. O., et al.: Phys. Rev. **C31**, 309 (1985)
43. Cameron, J. M., et al.: Nucl. Phys. **A458**, 637 (1986)
44. De Graeve, A.: Doctoral Thesis. Gent 1988
45. Meyer, H. O., et al.: Phys. Rev. Lett. **52**, 1759 (1984)
46. Levi Sandri, P., et al.: Preprint LNF-88/50 (P). Frascati 1988
47. Matone, G., et al.: In: Proceedings of International School of Intermediate-Energy Nuclear Physics, Verona (Bergère, R., Costa, S., Schaerf, C., eds.), p. 505. Singapore: World Scientific 1986
48. Ninane, A., et al.: Phys. Rev. **C35**, 402 (1987)
49. Barannik, V. P., et al.: Sov. J. Nucl. Phys. **38**, 667 (1983)
50. Vnukov, I. E., et al.: JETP Lett. **43**, 659 (1986)
51. Gorbenko, V. G., et al.: Sov. J. Nucl. Phys. **35**, 627 (1982)

Received July 24, 1989; accepted for publication September 1, 1989